

UNCLASSIFIED

AD NUMBER
AD005152
NEW LIMITATION CHANGE
TO Approved for public release, distribution unlimited
FROM Distribution authorized to U.S. Gov't. agencies and their contractors; Administrative/Operational Use; MAR 1953. Other requests shall be referred to National Aeronautics and Space Administration, Washington, DC.
AUTHORITY
NASA TR Server website

THIS PAGE IS UNCLASSIFIED

Reproduced by

Armed Services Technical Information Agency

DOCUMENT SERVICE CENTER

KNOTT BUILDING, DAYTON, 2, OHIO

AD -

5152

UNCLASSIFIED

NACA TN 2918

5152

NATIONAL ADVISORY COMMITTEE
FOR AERONAUTICS

TECHNICAL NOTE 2918

EFFECTS OF PARALLEL-JET MIXING ON DOWNSTREAM MACH
NUMBER AND STAGNATION PRESSURE WITH APPLICATION
TO ENGINE TESTING IN SUPERSONIC TUNNELS

By Harry Bernstein

Lewis Flight Propulsion Laboratory
Cleveland, Ohio



Washington
March 1953

TECHNICAL NOTE 2918

EFFECTS OF PARALLEL-JET MIXING ON DOWNSTREAM MACH NUMBER
AND STAGNATION PRESSURE WITH APPLICATION TO ENGINE
TESTING IN SUPERSONIC TUNNELS

By Harry Bernstein

SUMMARY

A one-dimensional analysis of the results of the parallel-jet mixing encountered in the testing of engines in supersonic wind tunnels is reported. Equations were derived for determining the total pressure and Mach number behind the tunnel terminal shock. The method represents a simple procedure for determining these quantities while a tunnel is still in the design stage. A specific example of the method is included.

INTRODUCTION

The results of mixing two streams of different temperatures, pressures, and Mach numbers are of importance in the wind-tunnel testing of engines. In a tunnel the exhaust gases of the engine mix with the tunnel air. The effect of such a mixing upon the total pressure and Mach number of the combined streams is of particular interest. The evaluation of these effects as functions of engine-performance parameters is of importance in determining the tunnel power requirements.

The present investigation, made at the NACA Lewis laboratory, is concerned with the analysis of the results of this mixing process by means of one-dimensional-flow equations. The analysis is restricted to the case in which the area of the resultant stream is equal to the sum of the areas of the original streams. As a result of this restriction, the solution is made dependent upon the upstream conditions only. The existence of any area changes would make it necessary to evaluate any axial forces and include them in the momentum equation. Such forces would be dependent upon the strengths and positions of any shocks in the mixing region; these in turn would be dependent upon the downstream static pressure.

The solution, when area changes exist, is therefore dependent, for a given set of upstream conditions, upon the downstream static pressure.

The solution as presented is also applicable to problems associated with the mixing in long cylindrical ejectors and to any other problems to which the restrictions made in the analysis apply.

SYMBOLS

The following symbols are used in this report:

- A stream cross-sectional area
- C_p specific heat of air at constant pressure
- H heating value of fuel, Btu/lb
- K ϕ_3/ϕ_1 , defined in eq. (9)
- M Mach number
- m_a air flow through engine, lb/sec
- m_f fuel mass-flow rate, lb/sec
- m_t total mass-flow rate of two streams being mixed, lb/sec
(mass of fuel not included)
- P total pressure
- p static pressure
- T total temperature, °R
- t static temperature, °R
- X defined in eq. (7)
- Y defined in eq. (8)
- α product of area and static pressure ratios of two streams being mixed, $A_2 p_2 / A_1 p_1$
- γ ratio of specific heats for air

- η_c combustion efficiency of engine, $\frac{\Delta T \text{ across combustion chamber}}{\text{maximum possible } \Delta T}$
- θ ratio of static temperatures in streams being mixed, t_2/t_1
- ξ ratio of Mach numbers of streams being mixed, M_2/M_1
- τ ratio of total temperatures in streams being mixed, T_2/T_1
- ϕ a function of Mach number, $\frac{M^2 \left(1 + \frac{\gamma - 1}{2} M^2\right)}{(1 + \gamma M^2)^2}$

Subscripts:

- m measured value (fig. 6)
- max maximum measured value (fig. 6)
- 0 conditions in engine inlet stream tube
- 1 conditions in tunnel stream adjacent to engine exit station
- 2 conditions in exhaust stream at engine exit station
- 3 conditions after mixing

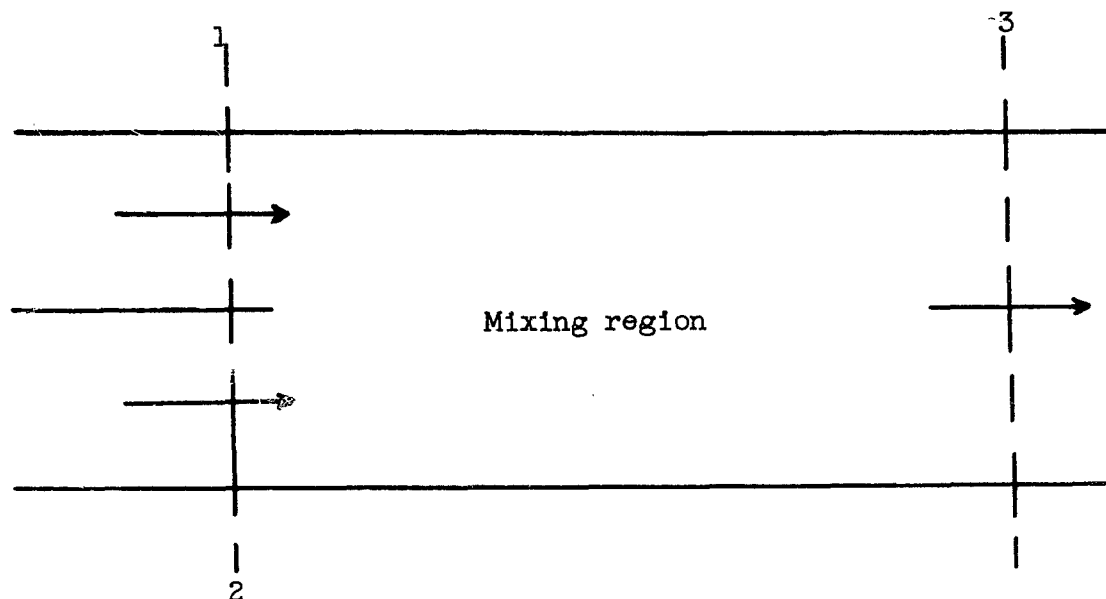
Superscripts:

- ' conditions behind normal shock (corresponding to unprimed conditions of same subscript ahead of shock)
- " conditions in resultant stream after heat addition in mixing region (corresponding to quantities of same subscript before heat addition)

MIXING EQUATIONS

Derivation

The analysis is restricted to the case of one-dimensional flow, where the area of the streams after mixing is equal to the sum of the areas of the two streams being mixed (see sketch). The momentum equation may contain no body force terms between the initial and final stations at which the flow is uniform.



The equations relating conditions before and after the mixing process are (since $A_1 + A_2 = A_3$):

Momentum equation

$$p_1 A_1 (1 + \gamma M_1^2) + p_2 A_2 (1 + \gamma M_2^2) = p_3 A_3 (1 + \gamma M_3^2) \quad (1)$$

Energy equation

$$p_1 A_1 \sqrt{t_1} M_1 \left(1 + \frac{\gamma - 1}{2} M_1^2 \right) + p_2 A_2 \sqrt{t_2} M_2 \left(1 + \frac{\gamma - 1}{2} M_2^2 \right) \\ = p_3 A_3 \sqrt{t_3} M_3 \left(1 + \frac{\gamma - 1}{2} M_3^2 \right) \quad (2)$$

Continuity equation

$$\frac{p_1 A_1 M_1}{\sqrt{t_1}} + \frac{p_2 A_2 M_2}{\sqrt{t_2}} = \frac{p_3 A_3 M_3}{\sqrt{t_3}} \quad (3)$$

The assumption of constant γ and C_p was made in order to avoid the necessity of a trial-and-error solution. The validity of this assumption is discussed in appendix A.

The effects of viscosity in the boundary layer along the wall of the channel (friction force) are neglected throughout this analysis.

In most tunnels suitable for engine testing, this force is small relative to the pressure and momentum changes of the main stream. The effects of viscosity and turbulence in the mixing process are irrelevant if conditions at station 3 are uniform, as assumed.

Division of each of equations (1), (2), and (3) by its first term yields

$$1 + \alpha X = \frac{p_3 A_3 (1 + \gamma M_3^2)}{p_1 A_1 (1 + \gamma M_1^2)} \quad (4)$$

$$1 + \alpha \xi Y \sqrt{\theta} = \frac{p_3 A_3 \sqrt{t_3} M_3 \left(1 + \frac{\gamma - 1}{2} M_3^2\right)}{p_1 A_1 \sqrt{t_1} M_1 \left(1 + \frac{\gamma - 1}{2} M_1^2\right)} \quad (5)$$

$$1 + \frac{\alpha \xi}{\sqrt{\theta}} = \frac{p_3 A_3 M_3 \sqrt{t_1}}{p_1 A_1 M_1 \sqrt{t_3}} \quad (6)$$

where α , ξ , and θ are defined as $\frac{A_2 p_2}{A_1 p_1}$, $\frac{M_2}{M_1}$, and $\frac{t_2}{t_1}$, respectively.

The parameters X and Y are defined as follows:

$$X = \frac{1 + \gamma \xi^2 M_1^2}{1 + \gamma M_1^2} \quad (7)$$

$$Y = \frac{1 + \frac{\gamma - 1}{2} \xi^2 M_1^2}{1 + \frac{\gamma - 1}{2} M_1^2} \quad (8)$$

Equations (4), (5), and (6) may be combined to eliminate the unknowns p_3 and t_3 , leaving M_3 as the only remaining unknown. Multiplying equations (5) and (6), dividing by the square of

equation (4), and setting $\frac{M^2 \left(1 + \frac{\gamma - 1}{2} M^2\right)}{(1 + \gamma M^2)^2} = \phi$ yields

$$\frac{(1 + \alpha \xi Y \sqrt{\theta}) \left(1 + \frac{\alpha \xi}{\sqrt{\theta}}\right)}{(1 + \alpha X)^2} = \frac{\phi_3}{\phi_1} = K \quad (9)$$

which shall be designated the mixing equation.

The known conditions at stations 1 and 2 and equation (9) are used to find the value of ϕ_3 . The function ϕ is plotted against Mach number in figure 1. The curves show that for values of ϕ greater than approximately 0.105, M is double-valued in ϕ . The two values of M are the supersonic and subsonic Mach numbers on either side of a normal shock. This may be shown analytically from a solution of the equations governing changes across a normal shock. As no restrictions were made in the derivation, it is inferred that (for the subsonic solution) the final conditions are independent of the order of occurrence of the processes of mixing and shock. In addition, the existence of only two solutions for the Mach number after mixing implies independence of the type of shock system in the mixing region.

To determine which value of M_3 is physically correct, three cases can be distinguished:

(a) The mixing streams are both subsonic. In this case the subsonic solution M_3 is always the correct one, since the supersonic solution will result in a net decrease in entropy.

(b) The mixing streams are both supersonic. In the mixing of two supersonic streams both solutions are physically possible. The supersonic solution will occur when the conditions require that the back pressure (static pressure after mixing) be low. If this back pressure is high, shocks will exist in the mixing region and the resultant stream will be subsonic. Choice of the solution is therefore dictated by the particular problem to which the results are applied.

(c) One stream is supersonic while the other is subsonic. In this case the subsonic solution is always possible. The supersonic solution is valid in cases where the subsonic jet is much smaller than the supersonic stream. The existence of such a supersonic solution is determined by an investigation of the entropy change in the process. If both solutions are possible, the choice is again dependent upon the particular problem under consideration.

In many instances the problem of mixing two streams of equal total temperature ($\tau = 1$) will arise. Here, since $\theta = \tau/\gamma$, equation (9) reduces to

$$K = \left(\frac{1 + \alpha \xi \sqrt{\gamma}}{1 + \alpha X} \right)^2 \quad (10)$$

When a solution for the Mach number after mixing has been obtained (either from eq. (9) or eq. (10)), substitution may be made in equations (4) and (6) to find p_3 and t_3 , respectively.

Discussion

The complexity of the mixing equation makes it difficult to determine, by inspection, the effects upon the resultant stream caused by variation in the values of each of the nondimensional parameters. In an effort to illustrate some of these effects, sample calculations for an M_1 of 3.0 were performed. The results are plotted in figures 2 and 3. The subsonic Mach number after mixing $M_{3,}$ is plotted in figure 2 as a function of the parameter α for a few chosen combinations of ξ and θ . The total-pressure ratio $P_{3,}/P_1$ is plotted in figure 3 as a function of the same independent variables. The combinations of ξ and θ were chosen to illustrate separately the effects of different Mach numbers and different static temperatures in the mixing streams.

As seen in figure 2, mixing streams of different temperatures ($\theta \neq 1$) caused an increase in the subsonic Mach number after mixing over the reference value ($\xi = 1, \theta = 1$; normal-shock solution for $M_1 = 3.0$). This increase is greatest at $\alpha = 1$, for any value of θ . As α approaches 0 or ∞ , the $M_{3,}$ curves approach the reference line asymptotically as would be expected, since these values of α imply that the area of one of the mixing streams is negligible with respect to the other.

The effects of mixing streams of different Mach number ($\xi \neq 1$) are observed to vary greatly with the value of ξ ; however, a few general conclusions about these variations may be stated. For any value of ξ , the curve is asymptotic to the reference line as α approaches zero. If a value of $\xi > 1$ is used, the resulting curve rises to a peak at some value of α less than unity. The curve then drops below the reference line and approaches a value of $M_{3,}$ asymptotically as α approaches ∞ . This value of $M_{3,}$ is the subsonic Mach number behind a normal shock at a Mach number M_2 ($M_2 = \xi M_1$). For $\xi < 1$, the curves rise above the reference line and reach a peak at some value of α larger than those values shown on the figure. (Differentiation of the mixing equation with respect to α shows that the curve of resultant Mach number has one peak for any values of ξ and θ , except the combination $\xi = 1, \theta = 1$.) As α approaches ∞ these curves are also asymptotic to some Mach number $M_{3,}$. This value is either the subsonic Mach number behind a shock at Mach number M_2 (for $M_2 > 1$), or M_2 itself (for $M_2 < 1$).

In the computations for the total-pressure ratios $P_{3,}/P_1$, some assumption had to be made concerning the variable α . While the Mach number curves (fig. 2) are quite general, the total-pressure-ratio

curves depend upon the actual components of α , that is, upon p_2/p_1 and A_2/A_1 (see eq. (4)). The ratio p_2/p_1 was therefore arbitrarily chosen to be unity, and hence α , in figure 3, represents the area ratio A_2/A_1 .

For $\xi = 1$ and different static temperatures ($\theta \neq 1$), the pressure-ratio curves (fig. 3(a)) fall below the reference line, become asymptotic to this line as α approaches 0 or ∞ , and have a minimum point at $\alpha = 1$. The decrease in total pressure is due to the heat exchange between the streams being mixed and the net entropy increase associated with this heat exchange.

For $\xi \neq 1$ (unequal Mach numbers), the curves (fig. 3(b)) are asymptotic to the reference line as α approaches zero. As α increases, the curves depart from the reference line, falling above or below it as ξ is greater than or less than unity, respectively. As α approaches infinity, these curves approach the values P_2/P_1 (for $M_2 = \xi M_1 > 1$) or P_2/P_1 (for $M_2 < 1$).

APPLICATION TO ENGINE TESTING IN SUPERSONIC WIND TUNNELS

The equations just derived may be applied in the design of a supersonic wind tunnel in which engines are to be tested. In such a tunnel the exhaust gases of the engine mix with the tunnel air; this mixing affects the values of the resultant Mach number and total pressure. The evaluation of the resultant stream properties as functions of engine-performance parameters is of importance in determining the power and pressure-ratio requirements of the tunnel. The arrangement is schematically illustrated in figure 4.

At the engine exit station, mean values of the flow properties of the tunnel stream (station 1) are required for the one-dimensional analysis. If A_2/A_0 is close to unity and the engine is operating at a mass-flow ratio of unity, these mean conditions may be taken as free-stream conditions. More accurate mean values may be obtained, if necessary, by constructing the flow field past the outer surface of the engine.

Flow properties in the exhaust jet at the engine exit (station 2) may be evaluated as functions of engine-performance parameters (P_2/P_0 , M_2 , τ). Again, the assumption of an engine operating at a mass-flow ratio of unity is made. If the mass of the fuel is neglected, the condition of constant mass flow yields the following relation between engine pressure recovery, exhaust-jet Mach number, and total-temperature ratio:

$$\left[\frac{\left(1 + \frac{\gamma - 1}{2} M_2^2\right)^3}{M_2} \right] = \frac{P_2}{P_0} \frac{A_2}{A_0} \left[\frac{\left(1 + \frac{\gamma - 1}{2} M_0^2\right)^3}{M_0} \right] \frac{1}{\sqrt{\tau}} \quad (11)$$

If the geometry of the engine to be tested (M_2 is a function of exhaust-nozzle geometry only) and τ are known, equation (11) provides a means of calculating the total pressure in the exhaust jet.

Once the conditions in the exhaust jet and the adjacent tunnel stream have been determined, use may be made of the mixing equation (eq. (9)) to evaluate tunnel Mach number and total pressure after mixing. For this application, station 3 must be assumed to be a suitable distance downstream of the tunnel terminal shock, and hence, the subsonic solution to the mixing equation is the proper solution. The reasons for this assumption are clearly illustrated in figures 5 and 6. Figure 5 shows a jet exhausting into a supersonic stream. The jet is observed to expand slightly to satisfy ambient static-pressure conditions, but little mixing is observed. This is further evidenced by the temperature profiles presented in figure 6. These profiles, which are affected by the amount of mixing, show that the major portion of the mixing occurs in a region downstream of the tunnel terminal shock, and hence the requirement that station 3 be a suitable distance downstream of the terminal shock.

Additional changes in Mach number and total pressure may be caused by heat addition in the mixing region. This is usually the case in engine testing, for excess fuel is carried out of the engine in the exhaust jet. This fuel burns in the mixing region just downstream of the tunnel terminal shock. Figure 7 illustrates this effect. Inasmuch as little fuel is usually carried out with the exhaust gas, as compared with the total mass-flow rate m_t , the magnitude of any changes due to this burning may be small, and in many cases can be neglected. In appendix B, relations are derived which may be used in evaluating the changes due to this heat addition, if a higher degree of accuracy is desired.

Throughout this analysis the tunnel terminal shock was assumed to be located in the test section downstream of the model. This represents peak efficiency operation of a tunnel having no second throat. While this is possible, most wind tunnels are not operated at peak efficiency but are operated with the terminal shock positioned a short distance downstream of the start of the tunnel diffuser. If this is the case, the results of this peak efficiency analysis must be corrected for the additional diffuser losses. In general, however, the trends indicated by this analysis will be unaffected. This constant-area analysis is not applicable for tunnels with second throats.

EXAMPLE

Consideration has been given to the problem of testing an engine having an 8-inch outlet diameter in an 18- by 18-inch tunnel operating at a Mach number of 3.1. To be found are the effects upon tunnel operating conditions caused by variations in τ and the exit-nozzle throat area of the engine being tested.

In this solution, the engine-air mass-flow ratio was assumed to be unity. Equation (11) was used to compute values of engine pressure recovery P_2/P_0 for various values of exit Mach number M_2 and τ . In order to simplify the problem, it was assumed that $A_2/A_0 = 1$ and that the engine was a perfect cylinder, making the conditions at stations 0 and 1 equal (see fig. 4).

With conditions at stations 1 and 2 known, the conditions in the tunnel after mixing were obtained by use of equations (9) and (4). The results of these computations are plotted in figures 8 and 9.

Figure 8 shows tunnel Mach number after mixing downstream of the normal shock in the test section M_3 , as a function of engine pressure recovery for various total temperature ratios. Lines of constant engine-exit Mach number are shown. Figure 9 shows resulting tunnel pressure recovery P_3/P_1 as a function of the same independent variables.

Increases in total-temperature ratio, while holding either M_2 or P_2/P_0 constant, result in higher values of M_3 and P_3/P_1 . An increase in the engine pressure recovery, while holding the total-temperature ratio constant, increases the tunnel pressure recovery and decreases the value of M_3 .

The increase in the tunnel pressure recoveries with increasing total-temperature ratios (greater heat addition) is explainable as follows. From the theory of one-dimensional gas flow (ref. 1), these facts may be stated about conditions at station 3': (1) At a constant value of total temperature, decreases in total momentum ($\rho A(1 + \gamma M^2)$) at this station will result in increased values of M_3 , and decreased tunnel pressure recovery P_3/P_1 , and (2) If total momentum is held constant, increases in energy will result in greater values of M_3 , and smaller tunnel recoveries.

In figures 8 and 9, lines of constant τ are lines of constant energy (constant T_3). Lines of constant total momentum ($\rho X = \text{constant}$) have been drawn on each figure. Larger values of

2814

αX are synonymous with greater total momentum at station 3' (eq. (4)), as station 1 represents tunnel free-stream conditions which are constant. If changes are observed along these energy and momentum lines, the results are seen to be in agreement with the one-dimensional gas-flow theory. Variations in P_3/P_1 with changes in fuel-air ratios are therefore an effect of combined momentum and energy changes.

CONCLUDING REMARKS

A one-dimensional analysis of the results of the parallel-jet mixing encountered in the testing of engines in supersonic wind tunnels has been reported. This type of analysis presents a reasonable approach to obtaining approximate figures for the tunnel operating conditions while the tunnel is still in the design stage. These figures would be based upon the known tunnel geometry and inlet conditions and estimations of the model geometry and values of the engine-performance parameters. Additional equations are presented for evaluation of changes due to the burning of excess fuel downstream of the engine-exhaust station.

In the evaluation of the properties of the engine-exhaust jet and the resultant (mixed) stream, it has been demonstrated that the assumptions of constant C_p and γ introduce no significant errors in the final results.

Lewis Flight Propulsion Laboratory
National Advisory Committee for Aeronautics
Cleveland, Ohio, January 5, 1953

APPENDIX A

DISCUSSION OF ERROR INVOLVED IN ASSUMPTION OF CONSTANT γ AND C_p

In view of the values of temperature associated with the testing of engines in supersonic wind tunnels and the variations of C_p and γ at these temperatures, the assumption of constant C_p and γ , as made in the mixing solution and in the determination of exhaust-jet properties, appears justified.

To illustrate, it is assumed that the total temperature of the exhaust jet is limited to a maximum of 3000°R , a value based approximately on the highest temperatures which present-day materials can withstand. It is also assumed that the exhaust-jet Mach number will be greater than or equal to 1.6, a reasonable value for an engine operating in a supersonic stream of moderate Mach number. These factors place an upper limit of approximately 2000°R on the static temperature of the exhaust stream, for an extreme case. It is to be realized that as the exhaust-jet Mach number increases or total temperature decreases or both, the value of its static temperature decreases.

In the usual supersonic wind tunnel, air is expanded to a temperature of the order of 200°R , although this figure may be decreased considerably for hypersonic tunnels. Hence, the range of static temperatures of importance in the mixing problem is from 200° to 2000°R . The mixed stream, prior to the tunnel terminal shock, would have a static temperature greater than, but much closer to, the 200°R figure, if supersonic mixing existed. This is a result of the small mass flow through the engine (hot air) as compared with that through the tunnel adjacent to the engine. The tunnel terminal shock may cause the static temperature to increase by a factor of 2 or 3, but a value of 2000°R is still felt to be an upper limit of static temperature in a very extreme case.

For air, the variations in C_p and γ are (ref. 2):

$t,$ $^\circ\text{R}$	$C_p,$ $\frac{\text{Btu}}{\text{lb-}^\circ\text{R}}$	γ
200	0.2395	1.400
500	.2400	1.400
1000	.2488	1.380
1500	.2644	1.349
2000	.2776	1.328

For 2000° R the variations in C_p and γ from the values of 200° R are 15.8 and 5.2 percent, respectively, although these variations decrease rapidly for temperatures less than 2000° R. In the range of temperatures from 200° to 540° R, both C_p and γ are constant.

To show the effects upon the accuracy of the results of the mixing problem when γ and C_p are assumed constant, the following problem was considered:

Tunnel size, 18 in. by 18 in.

Model size, 8 in. diam.

$$M_0 = 3.1$$

$$M_2 = 1.76$$

$$T_0 = 550^\circ \text{ R}$$

$$T_2 = 2370^\circ \text{ R}$$

$$\eta_c = 100 \text{ percent}$$

The exhaust-jet properties were found from these data, and then the mixing equations were applied, both with C_p and γ assumed constant and with values of C_p and γ dependent upon the temperature. The latter method involved a trial-and-error solution, the details of which are not presented here. A tabulation of results for both cases, along with percentage variations, follows:

	$C_{p,2}$	Variation in C_p , percent	γ_2	Variation in γ , percent	M_3	Variation in M_3 , percent	P_3/P_1	Variation in P_3/P_1 , percent
Constant C_p and γ	0.2400	9.6	1.400	3.4	0.580	2.6	0.3326	1.1
Variable C_p and γ	0.263		1.352		0.565		0.3288	

Large variations in C_p and γ are seen to result in very small variations in the final results.

2814

APPENDIX B

HEAT ADDITION IN MIXING REGION

The equation governing the flow of a fluid in a constant-area channel with heat addition can be written

Continuity equation

$$\frac{\rho M \sqrt{1 + \frac{\gamma - 1}{2} M^2}}{\sqrt{T}} = \frac{\rho'' M'' \sqrt{1 + \frac{\gamma - 1}{2} M''^2}}{\sqrt{T''}} \quad (B1)$$

Momentum equation

$$p(1 + \gamma M^2) = p''(1 + \gamma M''^2) \quad (B2)$$

Division of the continuity equation by the momentum equation yields

$$\left[\frac{M \sqrt{1 + \frac{\gamma - 1}{2} M^2}}{(1 + \gamma M^2)} \right] \sqrt{\frac{T''}{T}} = \left[\frac{M'' \sqrt{1 + \frac{\gamma - 1}{2} M''^2}}{(1 + \gamma M''^2)} \right] \quad (B3)$$

Equation (B3), when squared, becomes

$$\phi \left(\frac{T''}{T} \right) = \phi'' \quad (B4)$$

Application of this relation to the solution of the mixing problem yields

$$\phi_3 \left(\frac{T_3''}{T_3} \right) = \phi_3'' \quad (B5)$$

Therefore it is seen that ϕ_3'' can be directly obtained from ϕ_1 by the equation

$$\phi_3'' = K \left(\frac{T_3''}{T_3} \right) \phi_1 \quad (B6)$$

The ratio T_3''/T_3 is given in terms of fuel heating value and engine combustion efficiency as

2014

$$\frac{T_3''}{T_3} = 1 + \frac{(1 - \eta_c) \left(\frac{m_f}{m_t}\right) H}{C_p T_3} \quad (B7)$$

where

$$\frac{m_f}{m_t} = \frac{m_f}{m_a} \frac{m_a}{m_1} \frac{m_1}{m_t} = \frac{m_f}{m_a} \left(\frac{\alpha \xi}{\sqrt{\theta}}\right) \left(\frac{1}{1 + \frac{\alpha \xi}{\sqrt{\theta}}}\right) \quad (B8)$$

and

$$T_3 = T_1 \left(\frac{1 + \frac{\alpha \xi \tau}{\sqrt{\theta}}}{1 + \frac{\alpha \xi}{\sqrt{\theta}}} \right) \quad (B9)$$

Combining equations (B7), (B8), and (B9) yields

$$\frac{T_3''}{T_3} = \frac{(1 - \eta_c) \left(\frac{m_f}{m_a}\right) \left(\frac{\alpha \xi}{\sqrt{\theta}}\right) H}{C_p T_1 \left(1 + \frac{\alpha \xi \tau}{\sqrt{\theta}}\right)} + 1 \quad (B10)$$

The combustion efficiency η_c is given approximately as

$$\eta_c = \frac{(\tau - 1) C_p T_1}{\frac{m_f}{m_a} H} \quad (B11)$$

When ϕ_3'' has been evaluated, M_3'' may be obtained from figure 1. Choice of the subsonic or supersonic solution is determined by the same factors discussed in relation to equation (9) or supersonic wind tunnels.

The conservation of momentum and mass flow during the heat addition process allows the use of equations (4) and (6) for determining p_3'' and t_3'' , respectively, from the value of M_3'' .

A comparison of equations (9) and (B6) illustrates the effect of heat addition in the mixing region. Since T_3''/T_3 is always greater than unity for such a heat addition, then $\phi_3'' > \phi_3$, and hence

$M_3'' > M_3'$. Addition of heat in the mixing region therefore causes an increase in the subsonic Mach number at station 3. A further effect, as indicated in reference 1, is to cause an increase in the entropy of the stream, with a subsequent decrease in total pressure at station 3.

REFERENCES

1. Shapiro, Ascher H., and Hawthorne, W. R.: The Mechanics and Thermodynamics of Steady One-Dimensional Gas Flow. Jour. Appl. Mech., vol. 14, no. 4, Dec. 1947, pp. A317-A336.
2. Keenan, Joseph H., and Kaye, Joseph: Thermodynamic Properties of Air. John Wiley & Sons, Inc., 1945.

2814

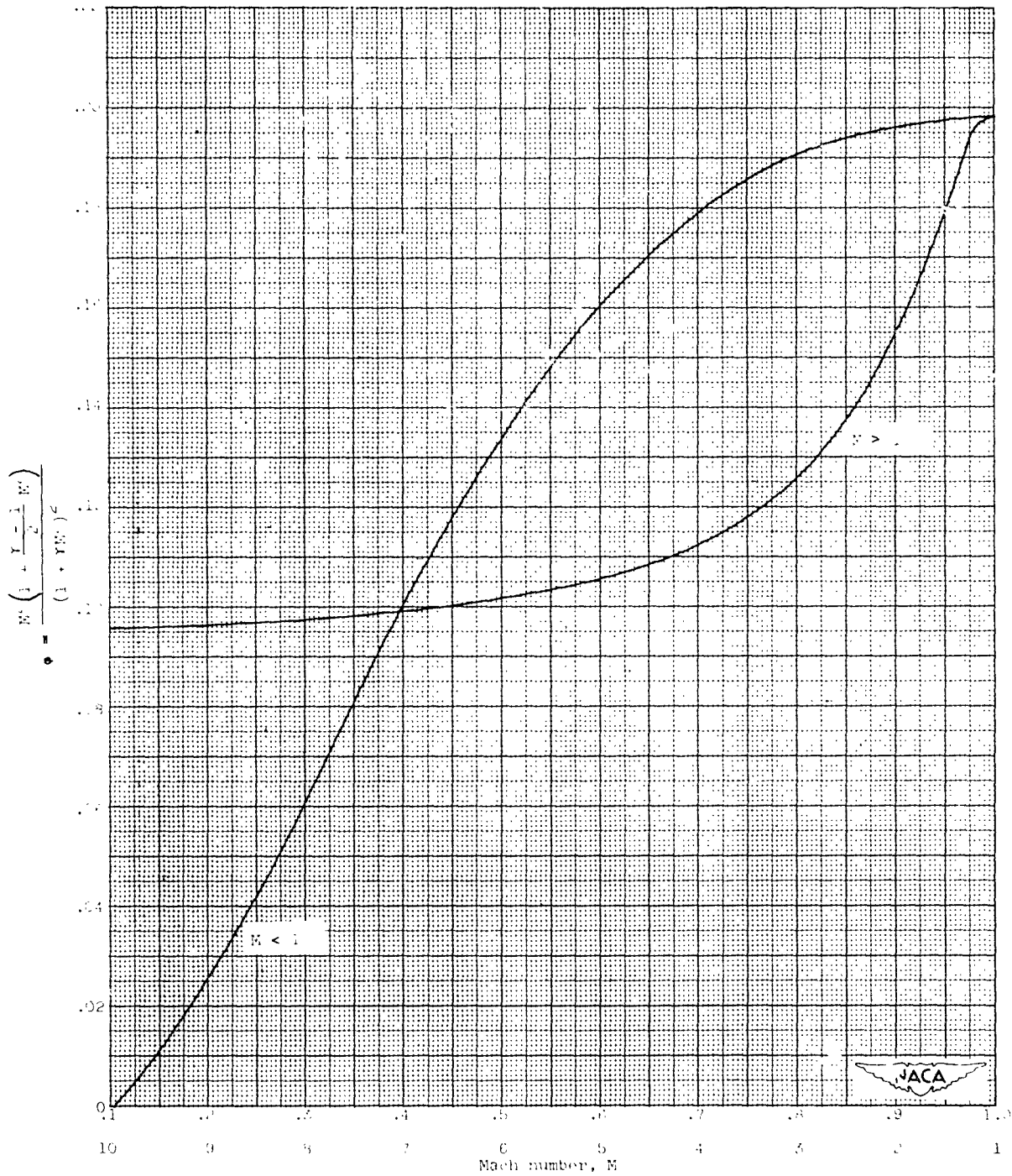


Figure 1. - Variation of function ϕ with Mach number for air (ratio of specific heats, 1.4).

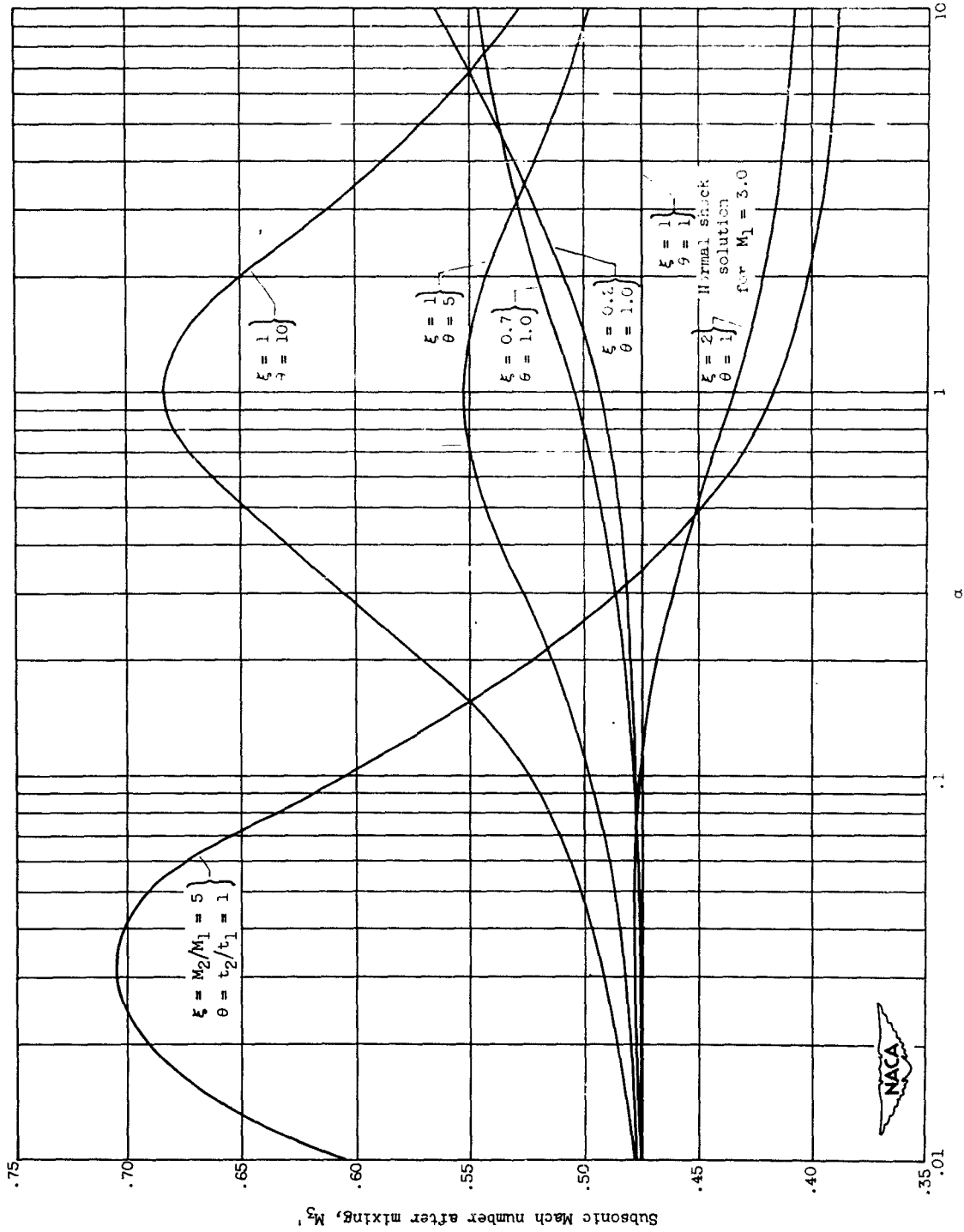
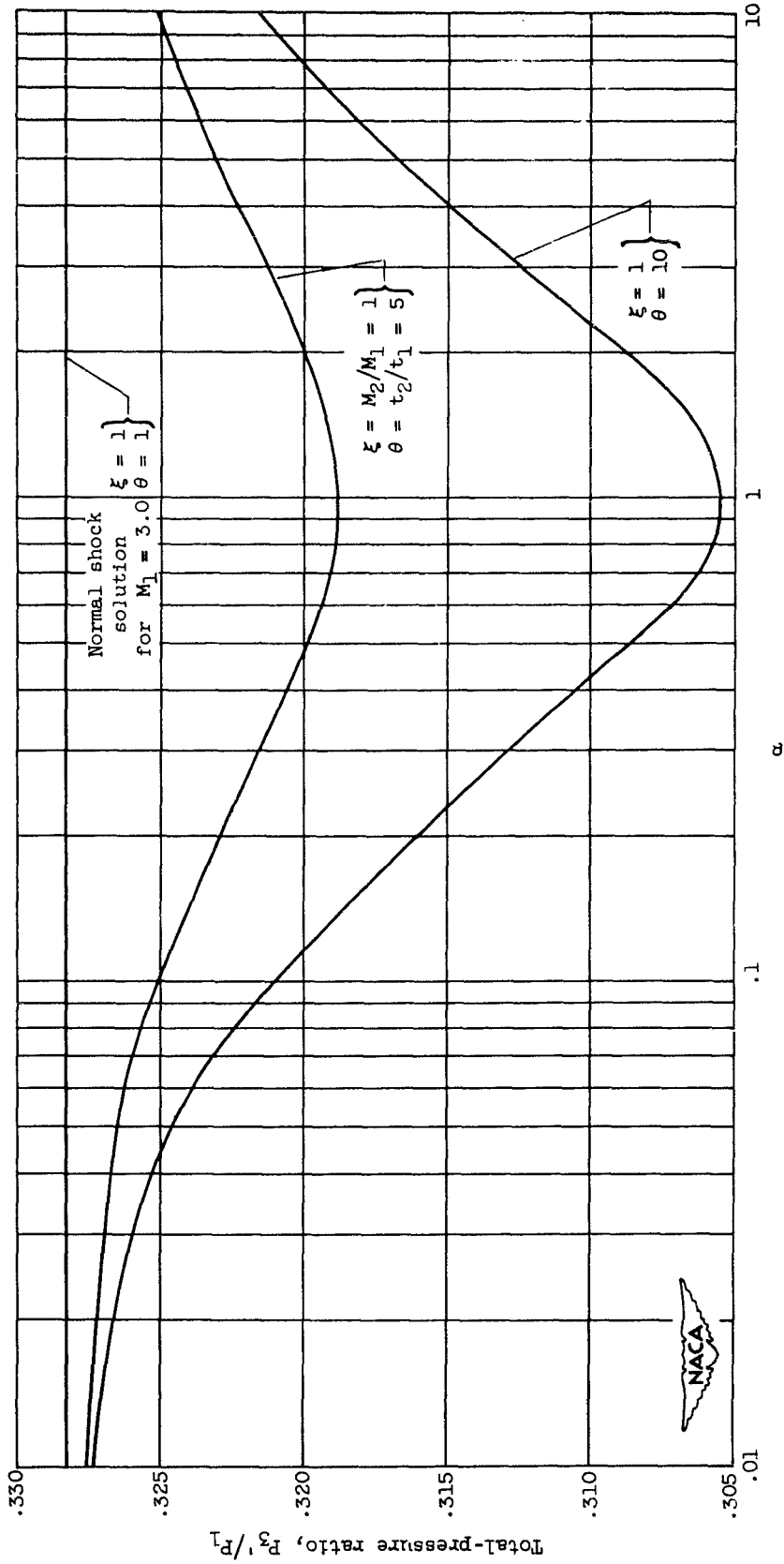


Figure 2. - Effect of variation in parameters of mixing equation on Mach number after mixing ($M_1 = 3.0$).

2814



(a) Ratio of Mach numbers of streams being mixed ξ equal to 1.
 Figure 3. - Effect of variation of parameters in mixing equation on total-pressure ratio of mixing process ($M_1 = 3.0$; $P_1 = P_2$).

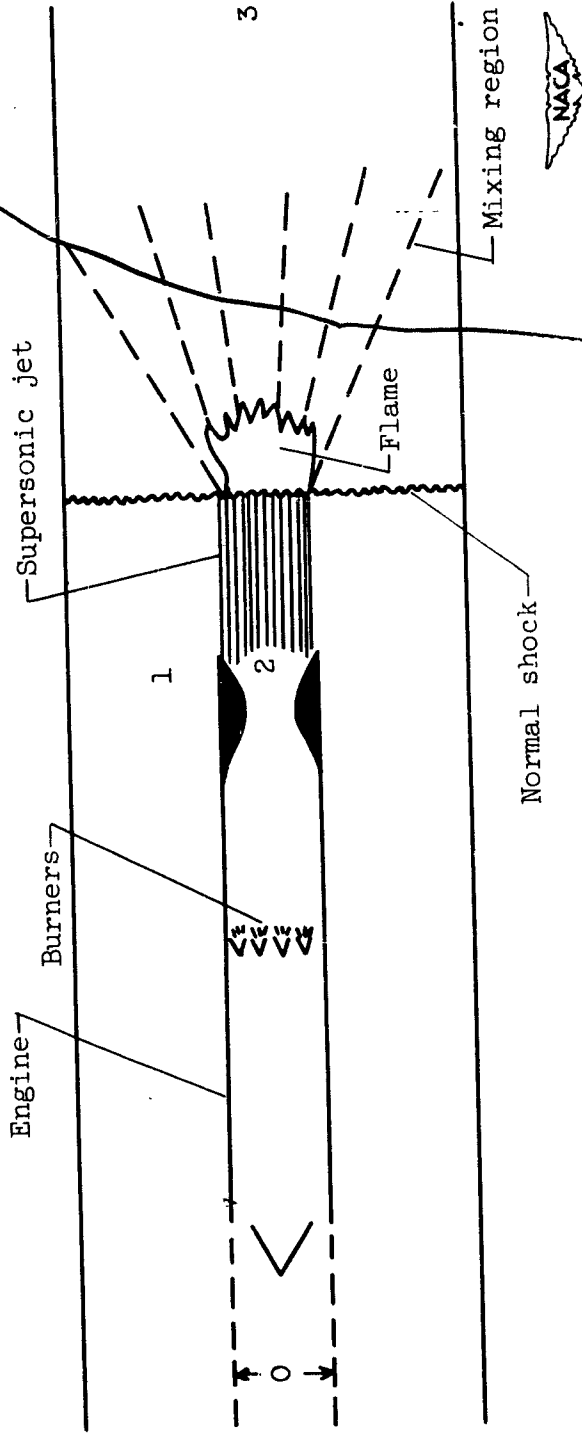


Figure 4. - Schematic illustration of engine being tested in supersonic wind tunnel.

2814

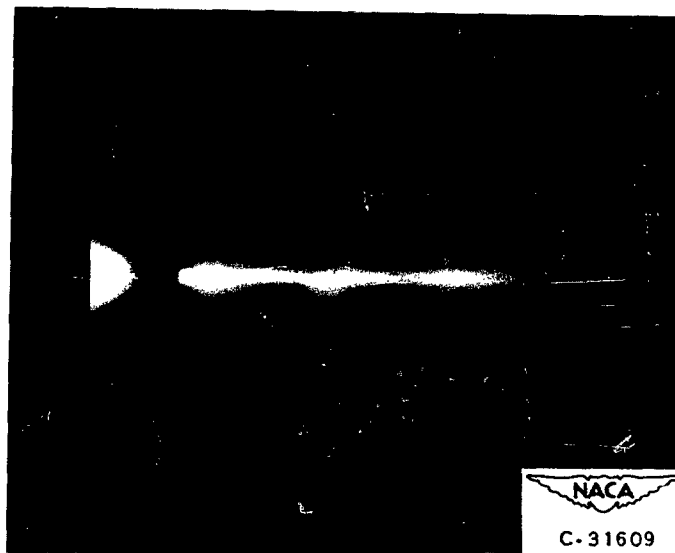


Figure 5. - Photograph of 5/8-inch-diameter jet exhausting at Mach number 1 into supersonic stream of Mach number 2.07.

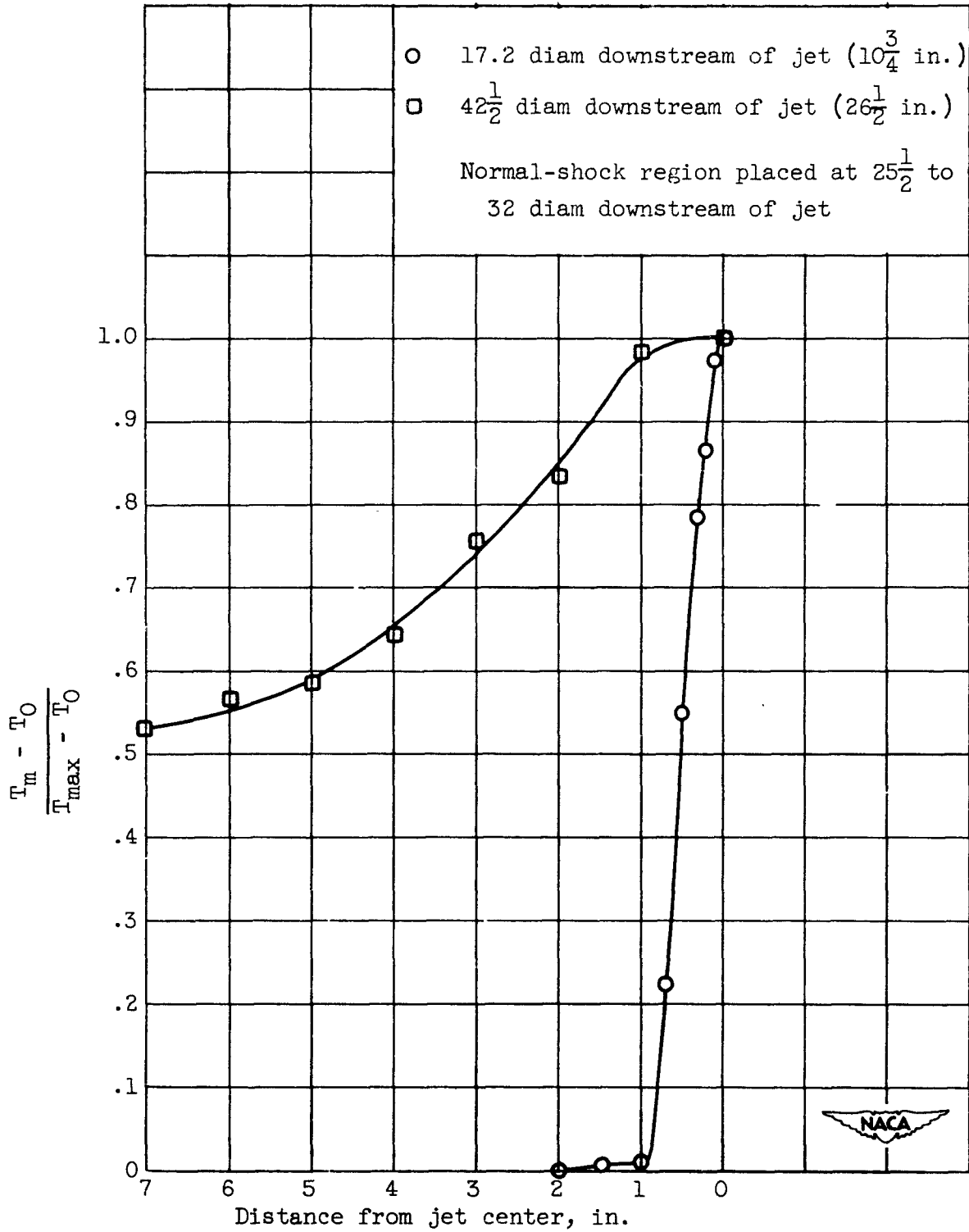
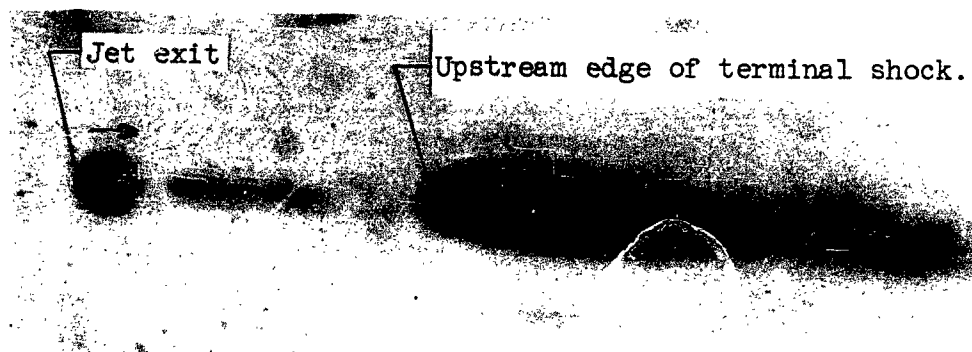
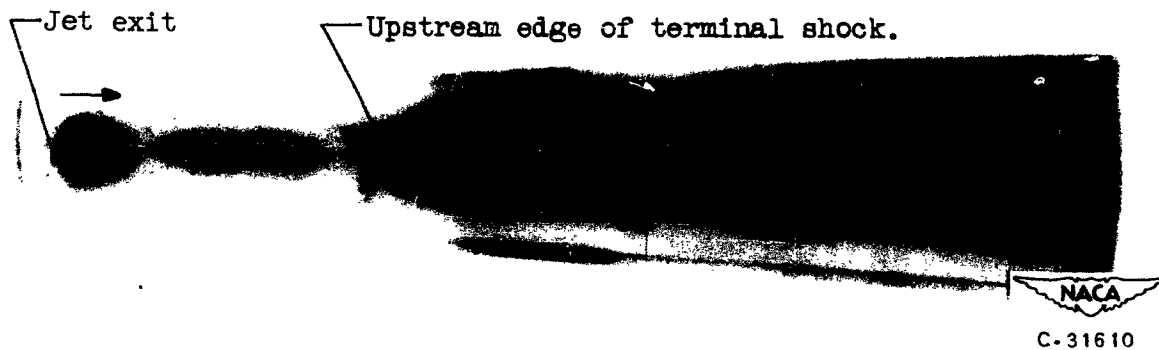


Figure 6. - Temperature profiles for jet shown in figure 5.



(a) Normal mixture ($m_f/m_a = 0.033$).



(b) Rich mixture ($m_f/m_a = 0.05$).

Figure 7. - Burning of excess fuel in region of tunnel terminal shock.

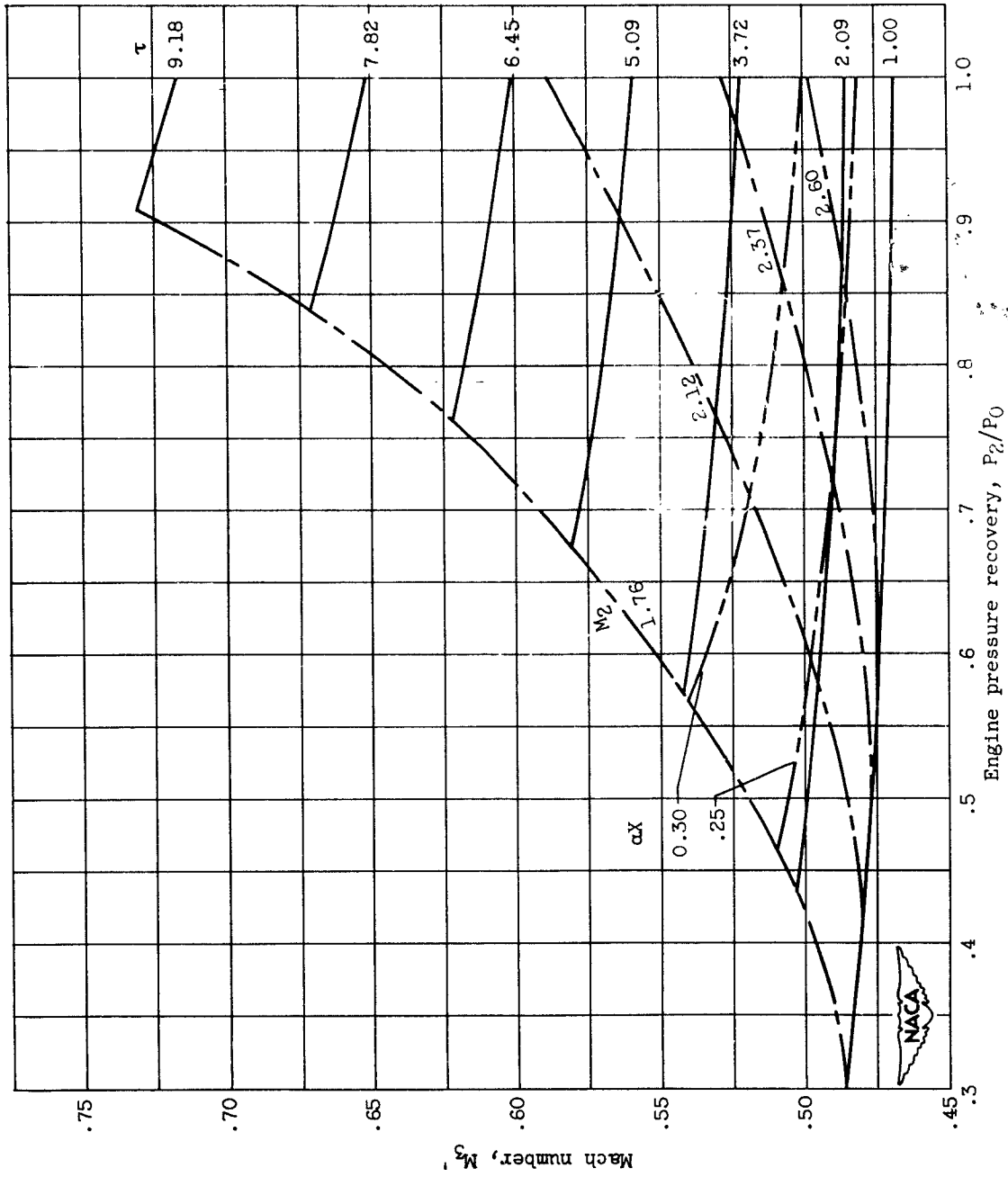


Figure 8. - Tunnel Mach number after mixing as a function of engine pressure recovery and total temperature ratio for constant engine mass flow. $M_1 = 3.1$; $A_2/A_1 = 0.1857$; $\gamma = 1.4$.

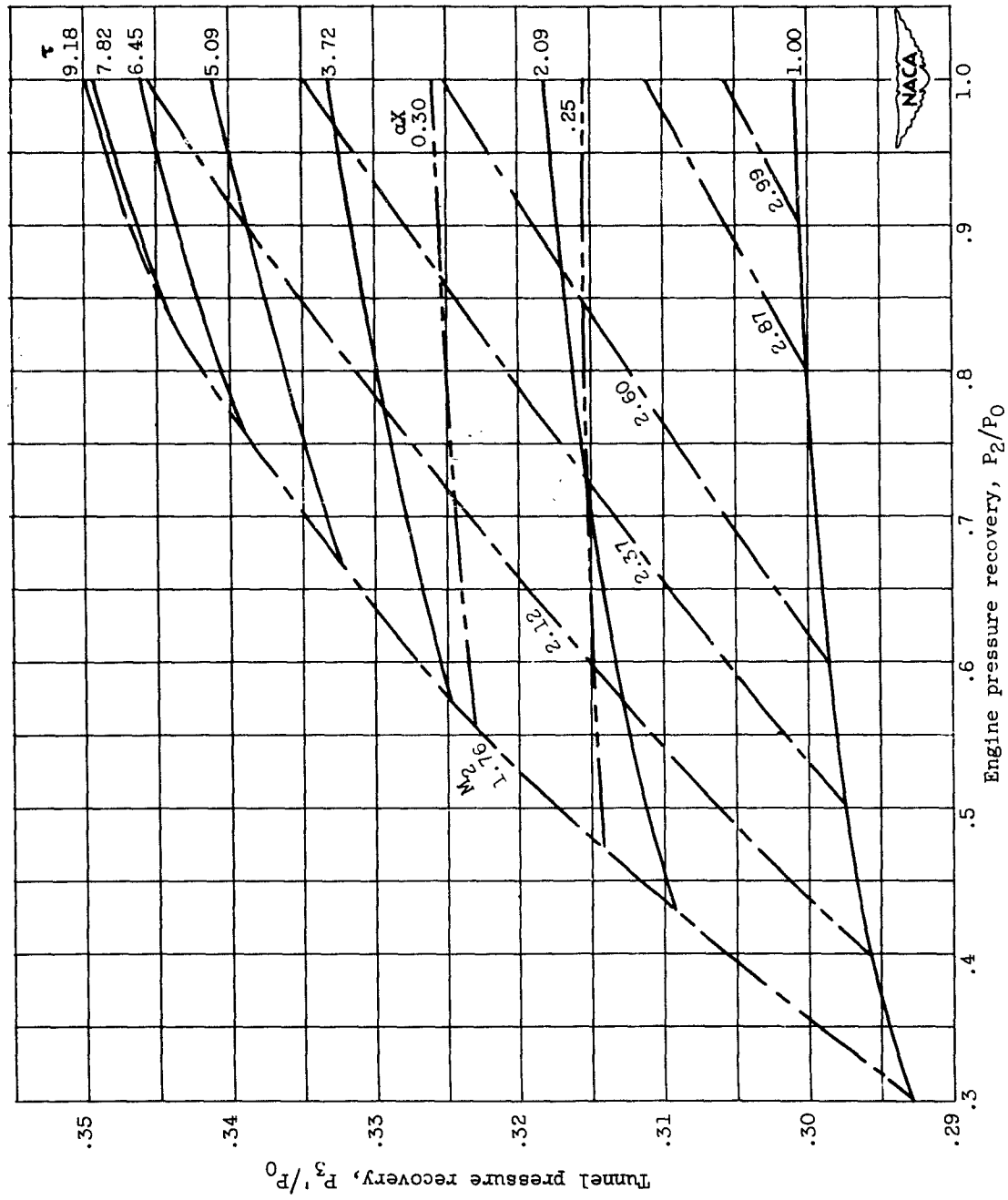


Figure 9. - Tunnel pressure recovery as a function of engine pressure recovery and total temperature ratio for constant engine mass flow. $M_1 = 3.1$; $A_2/A_1 = 0.1837$; $\gamma = 1.4$.